Thermodynamic assessment of the niobium-fluorine system by coupling density functional theory and CALPHAD approach

Capelli, E.; Konings, R. J.M.

DOI
10.1016/j.jfluchem.2018.01.011

Publication date
2018

Document Version
Accepted author manuscript

Published in
Journal of Fluorine Chemistry

Thermodynamic assessment of the niobium-fluorine system by coupling density functional theory and CALPHAD approach

E. Capelli[a,b,*], R. J. M. Konings[a,c]

[a] *Department of Radiation Science and Technology, Faculty of Applied Sciences, Delft University of Technology, Delft, 2629JB, The Netherlands*

[b] *Nuclear Research and Consultancy Group (NRG), 1755LE Petten, The Netherlands*

[c] *European Commission, Joint Research Centre, 76125 Karlsruhe, Germany*

Abstract

The complete thermodynamic description of the niobium-fluorine system is presented for the first time in this work. It results from a critical evaluation of the available experimental data and new thermodynamic calculations. In total, three niobium fluoride solid phases (NbF_3, NbF_4 and NbF_5) and seven gaseous species (NbF, NbF_2, NbF_3, NbF_4, NbF_5, Nb_2F_{10} and Nb_3F_{15}) have been considered during the assessment. Novel data for all the gaseous species were calculated combining Density Functional Theory (DFT), for the prediction of the molecular parameters, and statistical mechanical calculations, for the determination of the thermal functions (i.e. standard entropy and heat capacity). The developed thermodynamic model was found to correctly reproduce all the available experimental data and was used to calculate the Nb-F phase diagram, which is presented in this work as well.

Keywords: thermochemistry, niobium fluoride, Molten Salt Reactor, fission products

*Corresponding author. Tel.: +31-15-27-82163
Email address: e.capelli@tudelft.nl (E. Capelli)

1. Introduction

Understanding the chemistry of niobium in fluorine-containing environments is of primary importance for different industrial applications [1], and in particular for the development of nuclear technology. Nowadays, fluoride salts are under investigation with regards to their employment for an innovative type of fission reactor, the Molten Salt Reactor (MSR) [2, 3]. In this reactor type, the fissile and fertile material (e.g. ThF_4, UF_4) are dissolved in a fluoride matrix (e.g. LiF, LiF-BeF_2) which is constantly mantained in the liquid state during reactor operation. Niobium enters the system as a result of two different processes, namely as a product of the fission reaction during reactor operation and as a product of corrosion of structural materials at high temperature. The fate of this element and its influence on the fuel properties strongly depends on its chemical and physical state, which in turn depends on the reactor parameters such as temperature and redox (fluorine) potential. A thermodynamic database, including the main fission products and their fluoride phases, is under development and it serves as a tool to establish the performance and the safety of such innovative systems.

Thermochemical calculations have proved to be a very powerful method to predict the stable chemical phases of fission products under different conditions [4, 5]. However, reliable predictions are only attainable if the complete thermodynamic description of all the possible phases at equilibrium is available. Direct experimental measurements are not always possible, especially if the intermediate phases are difficult to synthesize in pure form or are very sensitive to moisture and air. A combination of ab-initio calculations and CALPHAD is applied for these systems, such as the presented niobium-fluorine system.

In this work, a review of the thermodynamic data available in literature on the niobium fluoride phases is presented. The thermodynamic properties of the stable compounds have been revised and novel data were calculated for the gaseous species combining density functional theory (DFT) and statistical mechanical calculations. In order to resolve the existent discrepancies found in literature, in particular on the vapour composition of stoichiometric NbF_5, three thermodynamic models were tested and the predictions were compared with the available experimental data. A consistent thermodynamic database was compiled based on the optimization results and was used to calculate the phase diagram of the Nb-F system, which is presented for the first time in this work.

2. Review of the stable niobium fluoride phases and their thermodynamic data

Stable fluoride condensed phases exists for niobium in each of the oxidation states from 3 to 5. All the compounds are solids at room temperature and are extremely sensitive to moisture and air. The only fluoride compound of niobium readily available is the pentafluoride NbF_5 [6, 7, 8], which is a white crystalline solid with melting

point at 353 K and boiling point at 508 K. Pure NbF_4 is a black non-volatile, very hygroscopic solid. Synthesis was obtained either by reduction of NbF_5 with Nb in a quartz container at 523 K [9] or by Si reduction [10]. In vacuum, NbF_4 is stable to approximately 548–598 K and at temperature greater than 623 K, disproportionation takes place rapidly [10]. Finally, NbF_3 is a dark-blue crystalline substance which was prepared for the first time in 1955 [11] by reacting $NbH_{0.7}$ with acqueous HF at 843 K.

Among the stable niobium fluorides, NbF_5 is the only compound whose thermodynamic properties have been directly experimentally determined. Brady et al. [12] measured the low temperature and the high temperature heat capacity of NbF_5 in the temperature range from 50 to 500 K. From their data, the standard entropy of formation $S^0(NbF_5, cr, 298\ K) = 160.25 \pm 3\ J{\cdot}K^{-1}{\cdot}mol^{-1}$ and the enthalpy of fusion $\Delta_{fus}H = 12.22 \pm 0.06\ kJ{\cdot}mol^{-1}$ at $T_{fus} = 348.6$ K were also derived. The latter value, which is calculated as the difference in enthalpy between the liquid and the solid phase at the melting point, is far less than the previously reported enthalpy of fusion of $35.98 \pm 2\ kJ{\cdot}mol^{-1}$ measured by Junkins et al. [7]. The recommended value for the enthalpy of formation, $\Delta_f H^0(NbF_5, cr, 298\ K) = -1813.76 \pm 0.6\ kJ{\cdot}mol^{-1}$, was taken from the work of Greenberg [13], who used fluorine combustion calorimetry, and agrees very well with the previous thermodynamic study by Myers and Brady [14], who used solution calorimetry.

The gaseous phase of the niobium-fluorine system can be described as an ideal mixture of several species, namely NbF(g), NbF_2(g), NbF_3(g), NbF_4(g), NbF_5(g) and $(NbF_5)_n$(g), with relative concentrations dependent on temperature and fluorine content. Although the presence of polymeric species of the pentafluoride in the gas phase is well established [15, 16, 17, 18], different degrees of polymerization were reported in literature and the interpretation of the results is sometimes contradictory. Brunvoll et al. [19] and Gotkis et al. [20] both identified the trimer as the main polymeric species using electron diffraction and mass spectrometry respectively. On the contrary, a recent study by Boghosian et al. [21] using Raman spectroscopy was in favor of a dimeric association at temperatures lower than 573 K. The main challenge for the interpretation of the spectra is given by the complex behaviour of the polymeric species as function of temperature. All the recent works [18, 21] agree on the presence of both monomer and polymers over stoichiometric NbF_5 with a strong temperature dependent concentration ratio. At low temperature, the polymer is the predominant species while at higher temperature the monomer becomes predominant. Finally, the stability of the various configurations was also studied theoretically using the discrete variational method [22]. The study concluded that a dynamic equilibrium is most probable between the monomers and the associates, of which the trimer is the most favorable.

The thermodynamic properties of gaseous NbF_5 have been provided in various data compilation [23, 24, 25, 26] whereas a very limited set of data exists on the thermodynamic properties of the other gaseous niobium fluorides [25, 27]. The calculated thermodynamic tables are based on early estimates of the molecular and spectro-

scopic parameters by Galkin [28] obtained on the basis of empirical relations and comparison with similar fluoride molecules.

It is evident from the reported literature review that the thermodynamic properties of the lower niobium fluorides, both in the condensed and gaseous phases, are not well established and require further investigation. Moreover, no thermodynamic data are available for the pentafluoride polymeric species, whose configuration seems not yet unambiguously solved.

3. Method

3.1. Thermodynamic modeling

The FactSage software [29] was used in this work to perform the required thermodynamic calculations and compute the Nb-F phase diagram. The binary system was optimized according to the CALPHAD method, which is based on the minimization of the total Gibbs energy of the system composed by all the phases at equilibrium.

For pure compounds, the Gibbs energy is defined as follows:

$$G(T) = \Delta_f H^0(298) - S^0(298)T + \int_{298}^{T} C_p(T)dT - T\int_{298}^{T}\left(\frac{C_p(T)}{T}\right)dT \qquad (1)$$

where $\Delta_f H^0(298)$ and $S^0(298)$ are respectively the standard enthalpy of formation and the standard absolute entropy, both referring to a temperature of 298.15 K. The $C_p(T)$ term is the temperature function of the heat capacity at constant pressure.

The properties for pure Nb and F_2 used in this work were taken from [30] while the selection of data for the NbF_5 condensed phases is discussed in the previous section. A simultaneous linear regression of the enthalpy data above room temperature and the heat capacity data at low temperature was applied to calculate the heat capacity function for the solid NbF_5. In this procedure, the value at 298.15 K was costrained at C_p=134.85 $J{\cdot}K^{-1}{\cdot}mol^{-1}$, as measured by Brady et al. [12].

No experimental data were found in literature on the thermodynamic properties of the lower solid niobium fluorides NbF_3 and NbF_4. In order to estimate their standard entropies and the heat capacity functions, a weighted average was applied starting from the properties of NbF_5 and Nb metal. This is equivalent to assume no entropy change and no change in the $C_p(T)$ function for the following generic reaction:

$$n\ NbF_5(cr) + (5-n)\ Nb(cr) \quad \longrightarrow \quad 5\ NbF_n(cr). \qquad (2)$$

In this case, the standard entropy and the standard heat capacity of the NbF_n species may be estimated from the following relations:

$$C_p^0(\mathrm{NbF_n}, cr, T) = \frac{1}{5}[n\ C_p^0(\mathrm{NbF_5}, cr, T) + (5-n)\ C_p^0(\mathrm{Nb}, cr, T)] \quad (3)$$

$$S^0(\mathrm{NbF_n}, cr, T) = \frac{1}{5}[n\ S^0(\mathrm{NbF_5}, cr, T) + (5-n)\ S^0(\mathrm{Nb}, cr, T)] \quad (4)$$

where $C_p^0(\mathrm{NbF_n}, cr, T)$, $C_p^0(\mathrm{NbF_5}, cr, T)$ and $C_p^0(\mathrm{Nb}, cr, T)$ are the standard heat capacity at temperature T of the considered solid lower niobium fluorides NbF_n, the NbF_5 and the metallic niobium, respectively. $S^0(\mathrm{NbF_n}, cr, T)$, $S^0(\mathrm{NbF_5}, cr, T)$ and $S^0(\mathrm{Nb}, cr, T)$ are the standard absolute entropies for the same compounds. It should be noted here that while this assumption is widely used for the determination of the properties of intermediate compounds starting from the end-members (Neumann-Kopp rule), it is seldom used in this form. In order to test the applicability of equations 3 and 4, the proxy compounds UF_4 and UF_3 were considered as their thermodynamic properties are well-established. Starting from the thermodynamic functions of solid UF_4 and metallic U, both taken from [31], the thermodynamic properties of UF_3 were determined. The standard entropy calculated with this method is equal to 126.38 $J{\cdot}K^{-1}{\cdot}mol^{-1}$ and compares extremely well with the literature value for UF_3 of 126.8± 2.5 $J{\cdot}K^{-1}{\cdot}mol^{-1}$ [32]. A good agreement was also found between the calculated heat capacity for UF_3 and the literature value [31] with a discrepancy of less than 5%. Finally, the enthalpy of formation of solid NbF_4 and solid NbF_3 were optimized in this work based on the experimental data on their thermal stability.

Table 1 summarizes the thermodynamic properties of the solid and liquid niobium fluorides considered in this work.

3.2. Statistical thermodynamic calculations

In contrast to the thermodynamic data of condensed phases which are either determined experimentally or estimated, the thermodynamic functions of gaseous species

Table 1: The thermodynamic properties $\Delta_f H^0(298)$ ($kJ{\cdot}mol^{-1}$), $S^0(298)$ ($J{\cdot}K^{-1}{\cdot}mol^{-1}$) and C_p($J{\cdot}K^{-1}{\cdot}mol^{-1}$) of solid and liquid niobium fluorides.

Compound	$\Delta_f\mathbf{H^0(298)}$	$\mathbf{S^0(298)}$	$\mathbf{C_p}$			
			a	**b·T**	**c·T^{-2}**	**T range**
NbF_3 (cr)	-1176.91	110.74	39.579	0.1718		298.15-352 K
			99.801	0.0017		352-3500 K
NbF_4 (cr)	-1517.67	135.49	45.117	0.2271		298.15-352 K
			125.13	0.0009		352-3500 K
NbF_5 (cr)	-1813.76	160.25	54.527	0.2744	-134780	298.15-352 K
NbF_5 (liq)	-1799.50	200.63	150.60			352-3500 K

may be calculated theoretically if the energy states of the molecules are known. The method is based on the computation of the partition function Q of the molecule and its derivative as function of temperature, which are then related to the thermodynamic functions of the system. In this work, the rigid-rotor/harmonic-oscillator approximation was used to express the intramolecular component of the partition function as a sum of indepedent components, namely the components of the harmonic oscillator and the rigid rotator. In the most general case of a non-linear polyatomic molecule, the mathematical expressions for the electronic, vibrational, rotational and translational components are given in Table 2. No corrections for anharmonic vibrations are applied.

The calculations were performed in this work by using a set of Fortran codes [33]. The computer program takes as input the molecular parameters and the spectroscopic data of the molecule, i.e the selected principal moment of inertia, the symmetry number, the vibrational frequencies and the low-lying electronic levels.

3.3. DFT computational details

The structure and the molecular parameters of the gaseous species were calculated in this work ab-initio using Gaussian09 code [34]. The hybrid DFT method B3LYP was applied, in which the Becke three-parameter exchange functional [35] and the Lee-Yang-Parr correlation functional [36] are used. The method was initially selected based on literature works ([37] and references therein), in which the B3LYP was found to provide reliable results for the transition metal series of elements. Some test calculations using different methods (i.e. PBE1PBE, BLYP, PBEPBE, M062X) were also performed on similar molecules for which experimental data exist, such as MoF_6. The best agreement in terms of both Mo-F interatomic distance (r_{calc}= 1.8287 Å; r_{exp}=1.82 Å [30]) and vibrational frequencies was indeed obtained with the B3LYP method. The small-core quasi-relativistic pseudopotentials of the Stuttgart-Cologne group for the metals (ECP28MWB for niobium with valence basis 8s7p6d2f1g/6s5p3d2f1g [38, 39]) and the cc-pVTZ all-electron basis set for fluorine [40] were considered in the present calculations.

The geometry optimizations were followed by frequency calculations at the optimized structure (Freq keyword in Gaussian09), which provide the moments of inertia and the harmonic oscillator frequencies of the molecules. Molecular energies can also be evaluated ab initio as function of the molecular geometry and are used to derive the standard enthalpy of formation of the gaseous compounds. The theoretical enthalpies of formation at 0 K are calculated as follows:

$$\Delta_f H^0(NbF_x, 0\text{ K}) = \Delta_f H^0(Nb, 0\text{ K}) + x \cdot \Delta_f H^0(F, 0\text{ K}) - \sum D_0 \quad (5)$$

where $\sum D_0$ is the atomization energy of the molecule calculated from the output of the thermochemistry routine of Gaussian [41] at standard pressure while $\Delta_f H^0(Nb, 0\text{ K})$ and $\Delta_f H^0(F, 0\text{ K})$ are the standard enthalpy of formation of the isolated atoms Nb(g) and F(g) at 0 K, taken from [30]. For consistency within

Table 2: Mathematical expression of the electronic, vibrational, rotational and translational contribution to the entropy S^0 and heat capacity C_p^0 functions of a generic non-linear polyatomic molecule.

Intramolecular component	**Mathematical expression**
Translational	$C_p^0/R = \frac{5}{2}$ $S^0/R = \frac{3}{2}\ln M_r + \frac{5}{2}\ln T + \frac{5}{2} + \ln\frac{k}{p^0}\left(\frac{2\pi k}{Nh^2}\right)^{3/2}$
Electronic	$C_p^0/R = T^2\frac{\mathrm{d}^2 \ln Q}{\mathrm{d}T^2} + 2T\frac{\mathrm{d}\ \ln Q}{\mathrm{d}T}$ $S^0/R = T\frac{\mathrm{d}\ \ln Q}{\mathrm{d}T^2} + \ln Q$ where $Q = \sum_i g_i \mathrm{e}^{(-c_2\epsilon_i/T)}$
Rotational	$C_p^0/R = \frac{3}{2}$ $S^0/R = \frac{3}{2} + \frac{1}{2}(I_A I_B I_C) - \ln\,\sigma + \frac{3}{2}\ln\,T + \left(-\frac{3}{2}\ln\frac{h^2}{8R\pi^0} + \frac{1}{2}\ln\pi\right)$
Vibrational	$C_p^0/R = \frac{u^2\mathrm{e}^{-u}}{(1-\mathrm{e}^{-u})^2}$ $S^0/R = \frac{u\mathrm{e}^{-u}}{(1-\mathrm{e}^{-u})} - \ln(1-\mathrm{e}^{-u})$ where $u = c_2\omega/T$

Symbols: M_r: molecule molar mass; T: temperature; R: molar gas constant; Q: partition function; k: Boltzmann constant; p^0: pressure of standard state; h: Planck constant; N: number of atom in a molecule; g_i: statistical weight of the i^{th} level; c_2: second radiation constant; ϵ_i: energy of the electronic level; $I_A I_B I_C$: principal moment of inertia; σ: symmetry number; ω: fundamental frequency of the harmonic oscillator.

the database, the enthalpy of formation at 298.15 K were calculated applying the enthalpy correction for the molecule, as given in the Gaussian output, and for the elements taken directly from standard tables.

4. Results and discussion

4.1. Gaseous phases molecular parameters and structure

Seven niobium fluoride gaseous species have been studied in this work using density functional theory. The optimized geometries, which represent the minimum structure on the potential energy surfaces of the target molecules, are shown in Figure 1. For each of the studied molecules, different states of the ground energy level were tested according with the possible number of unpaired electrons which define the multiplicity of the energy level. Only the configurations having the lowest energy are reported in Table 3. Moreover, the ground state character of the final configuration was confirmed by checking for eventual lower energy solutions of the wave function.

The symmetry point groups and the bond lenghts as reported by Galkin [25] were used as initial values for the geometry optimization. The calculated interatomic distances Nb-F for all the gaseous species were found to be slightly lower compared to the initial estimations and, in some cases, the results of the DFT calculations lead to a change in the molecular symmetry point group. In case of the NbF_3 molecule, any attempt to fit the C_{3v} geometry rapidly converged to the planar form (D_{3h}) which was therefore preferred. NbF_4 was found to have lower than regular tetrahedral symmetry (D_{2d}) due to the distortion of the bond angles from the perfectly symmetric structure (109.47°) but still preserving the bond lenght equality.

The vibrational modes of the molecules were also calculated and are reported in Table 4 for the lower niobium fluorides NbF, NbF_2, NbF_3 and NbF_4. A more detailed discussion is required for NbF_5 and its polymeric species given the number of experimental and computational studies present in literature. As mentioned before, several models were proposed for the composition of niobium pentafluoride in the gas phase: monomers of D_{3h} [43] or C_{2v} symmetry [16], dimers of D_{2h} symmetry [21] and trimer of D_{3h} symmetry [19, 20]. All the configurations were studied in this work to improve the understanding of the system and to support the interpretation of the available experimental data. The D_{3h} symmetry model was confirmed in our calculations for the NbF_5 molecule and the corresponding frequencies are listed in Table 5. The results compare well with the experimental values (only Raman active modes) obtained by Alexander [16] and by Boghosian et al. [21].

As regards the polymeric species, both the dimeric model with D_{2h} symmetry and the trimeric model with D_{3h} symmetry were tested. In both configurations, the calculated molecular parameters (i.e. the interatomic distances and angles) are close to the one obtained from electron diffraction studies [19]. Tight convergence

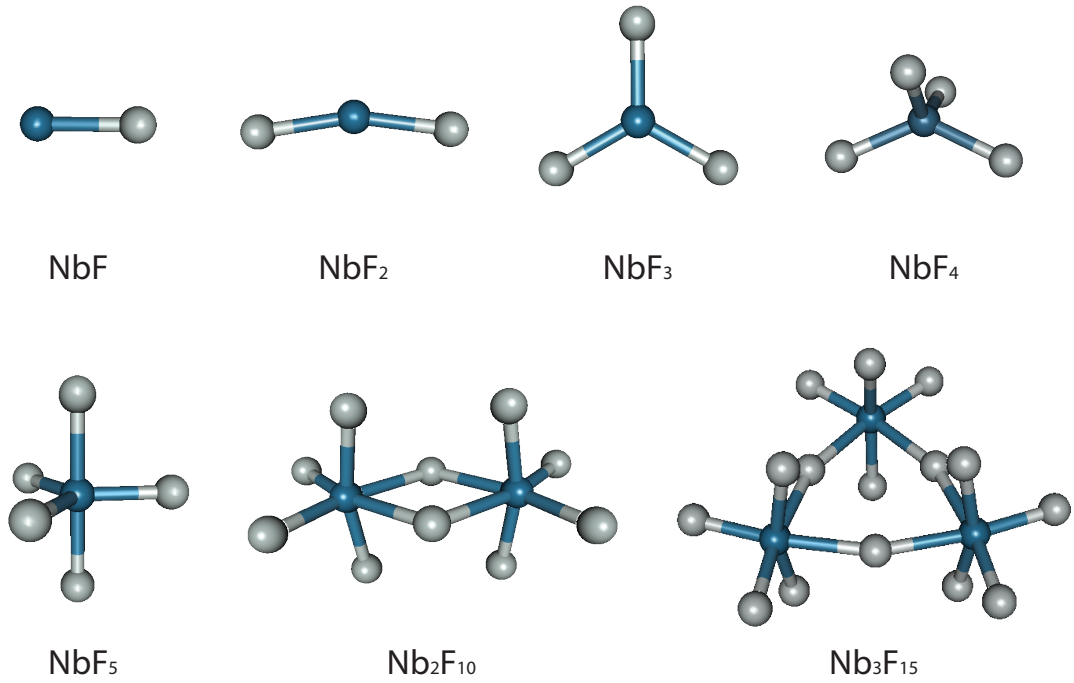

Figure 1: Geometrical configuration of the various niobium fluoride gaseous species optimized in this work and plotted with Gabedit software [42].

Table 3: The molecular parameters calculated in this work for the stable gaseous species NbF, NbF_2, NbF_3, NbF_4, NbF_5, Nb_2F_{10} and Nb_3F_{15}: symmetry point group, symmetry number σ, interatomic distances R (Nb-F) (Å), interatomic angles $\angle$ (F-Nb-F) (deg), calculated product of the principal moments of inertia $I_A I_B I_C$ (10^{111} g^3·cm^6) and ground state multiplicity n. The subscripts t, a and b denote the terminal, axial and bridged fluorine atoms respectively.

Parameters	**NbF**	**NbF_2**	**NbF_3**	**NbF_4**	**NbF_5**	**Nb_2F_{10}**	**Nb_3F_{15}**
Point group	C_v	C_{2v}	D_{3h}	D_{2d}	D_{3h}	D_{2h}	D_{3h}
$\boldsymbol{\sigma}$	1	2	6	4	6	4	6
$\boldsymbol{R}$ **(Nb-F)**$_t$	1.8837	1.8812	1.8456	1.8672	1.8426	1.8334	1.8340
$\boldsymbol{R}$ **(Nb-F)**$_a$					1.8745	1.8596	1.8575
$\boldsymbol{R}$ **(Nb-F)**$_b$						2.1054	2.0916
$\angle$ **(F-Nb-F)**$_t$		162.87	120	99.86	120	103.37	98.34
$\angle$ **(F-Nb-F)**$_a$				131.12		70.08	81.83
$\angle$ **(F-Nb-F)**$_b$						167.79	165.16
$\mathbf{I_A I_B I_C}$	n/a*	$1.703{\cdot}10^{-3}$	8.376	9.010	$4.699{\cdot}10^{-2}$	5.360	94.723
n	5	4	1	2	1	1	1

* Spectroscopic constant B_0= 0.3012.

Table 4: The calculated vibrational frequencies of the lower niobium fluoride gaseous species NbF, NbF_2, NbF_3 and NbF_4. The assignment is based on the optimized geometries and the symmetry group calculated in this work.

Molecule	**Frequencies / cm^{-1} (Assignment)**
NbF	645.91 **(fundamental)**
NbF_2	111.1 ($\mathbf{A}_1$); 644.4 ($\mathbf{A}_1$); 682.0 ($\mathbf{B}_2$)
NbF_3	134.7 ($\mathbf{A}_2''$); 181.9 ($\mathbf{E}'$); 680.1 ($\mathbf{A}_1'$); 752.2 ($\mathbf{E}'$)
NbF_4	152.2 ($\mathbf{E}$); 154.2 ($\mathbf{A}_1$); 178.9 ($\mathbf{B}_2$); 190.6 ($\mathbf{B}_1$); 654.9 ($\mathbf{B}_2$) 682.8 ($\mathbf{A}_1$); 706.5 ($\mathbf{E}$)

Table 5: The vibrational frequencies of the NbF_5 gaseous molecule based on D_{3h} symmetry. Γ_ν: $2A_1'$ (R) + A_2'' (IR) + E′ (R,IR); Γ_γ: A_2'' (IR) + 2E′(IR, R) + E″(R)

Method (Ref.)	$\nu_1(\mathbf{E}')$	$\nu_2(\mathbf{A}_1')$	$\nu_3(\mathbf{A}_2'')$	ν_4 $(\mathbf{A}_1')$	$\nu_5(\mathbf{E}'')$	$\nu_6(\mathbf{A}_2'')$	$\nu_7(\mathbf{E}')$	$\nu_8(\mathbf{E}')$
Estimation [25]	726	767	688	683	349	510	253	226
Raman spec. [16]		727						
Raman spec. [21]		726			268		223	101
DFT [This work]	735.9	720.3	700.5	625.2	273.8	251.5	219.9	95.1
Selected	735.9	726	700.5	625.2	268	251.5	223	101

criteria had to be used in the calculation of these species in order to avoid very low-frequency modes, which would lead to a very high entropy value. The calculated frequencies of the Nb_2F_{10} and Nb_3F_{15} molecules are both reported in Table 6 and are compared with some selected experimental vibrational frequencies measured by IR [18, 16] and Raman spectroscopy [16, 21]. While the terminal stretching modes around 700 cm^{-1} agree quite well with both the dimeric and the trimeric association (similar octahedral NbF_6 unit), a larger discrepancy have been observed for the Nb-F bridged stretching modes around 500 cm^{-1}. In particular, the Nb_2F_{10} molecule shows no vibrational frequencies in the region around 510 cm^{-1}, which was reported as a broad absorption band by most of the authors [16, 18, 43, 44]. The IR spectra for the dimer and the trimer have been calculated based on the DFT results and are compared with the experimental data reported by Konings [18] at 320 K. As shown in Figure 2, a better agreement between the model and the experimentally measured frequencies is observed for the Nb_3F_{15} configuration, suggesting that the trimer is the main polymeric species for the given experimental conditions.

A list of selected vibrational modes for the NbF_5 and the Nb_3F_{15} gas molecules, used for the calculation of the thermodynamic properties, are reported in Table 5 and Table 6. When the interpretation of the results clearly indicated one predominant species, the experimental values have been preferred.

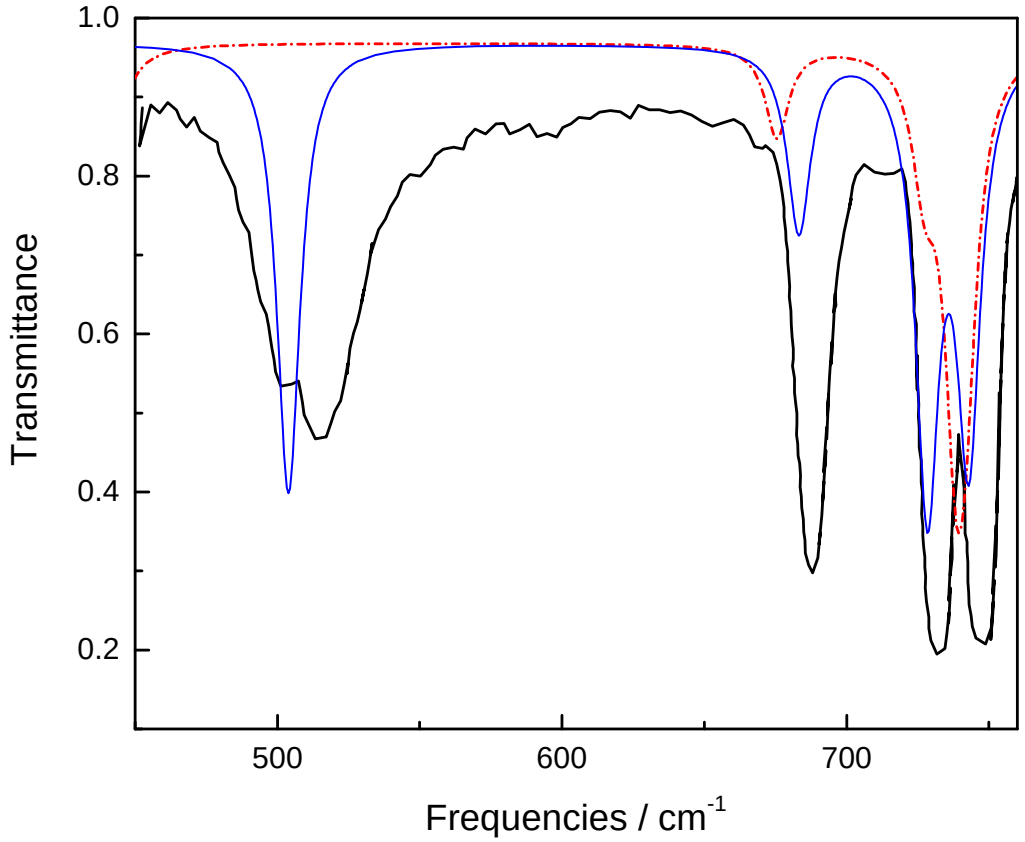

Figure 2: The calculated infrared spectrum of the gaseous molecules Nb_2F_{10} (red dash-dotted line) and Nb_3F_{15} (solid blue line) as optimized in this work. Solid black line: Digitized infrared spectra of the vapour above NbF_5(cr) as measured in [18] at 320 K.

Table 6: The vibrational frequencies of the Nb_2F_{10} and Nb_3F_{15} gaseous molecules based on the D_{2h} and D_{3h} symmetry, respectively. Γ (D_{2h}): 6 A_g (R) + 2A_u + 4 B_{1g} (R) + 4 B_{1u} (IR) +3 B_{2g} (R) +4 B_{2u} (IR)+2 B_{3g} (R)+ 5 B_{3u} (IR); Γ (D_{3h}): 6 A_1' (R) + 2A_1'' + 4 A_2' + 4 A_2'' (IR) +10 E′ (R,IR)+ 6E″ (R);

Calculated frequencies		**Measured frequencies**			**Selected**
Nb_2F_{10}	**Nb_3F_{15}**	**Raman 525-700 K [21]**	**Raman/IR 503-673 K [16]**	**IR 300-350 K [18]**	**Nb_3F_{15}**
746.3 (**A_g**,R)	752.1 (**A_1'**,R)	756	757 (R)		752.1
741.9 (**B_{1u}**,IR)	742.9 (**A_2''**,IR)		749 (IR)	747.8	748.5
738.4 (**B_{2u}**,IR)	738.6 (**E′**,IR/R)		734 (IR)	732.8	733.5
727.4 (**B_{3u}**,IR)	728.3 (**E′**,IR/R)				728.3
725.0 (**B_{2g}**,R)	713.6 (**A_2'**)				713.6
701.6 (**B_{1g}**,R)	709.6 (**E″**,R)				709.6
677.8 (**A_g**,R)	683.3 (**E′**,IR/R)		687 (R); 689 (IR)	687.5	687.5
675.6 (**B_{3u}**,IR)	681.1 (**A_1'**,R)	683			681.1
473.1 (**A_g**,R)	503.9 (**E′**,IR/R)		510 (IR)	502; 514	510.0
438.9 (**B_{3u}**,IR)	425.3 (**A_2'**)				425.3
365.3 (**B_{1u}**,IR)	315.9 (**A_2''**,R)				315.9
352.8 (**B_{2g}**,R)	299.6 (**E″**,R)				299.6
316.8 (**B_{2u}**,IR)	293.3 (**A_1'**,R)				293.3
281.6 (**B_{3g}**,R)	274.5 (**A_1'**,R)				274.5
265.0 (**A_g**, R)	271.1 (**E′**,IR/R)				271.1
249.9 (**B_{1g}**, R)	244.4 (**E″**,R)	253	252 (R)		244.4
249.1 (**B_{2u}**, IR)	243.1 (**A_2''**,IR)				243.1
238.6 (**A_u**)	229.0 (**A_1''**)				229.0
216.7 (**B_{3u}**,IR)	221.6 (**E′**, IR/R)			229	229.0
187.1 (**B_{3g}**,R)	202.4 (**E″**, R)	213	210 (R)		202.4
181.0 (**B_{1u}**,IR)	188.6 (**E′**,IR/R)				188.6
161.7 (**A_g**,R)	165.1 (**A_1'**,R)	170	170 (R)		165.1
159.3 (**B_{1g}**,R)	145.0 (**E′**,IR/R)				145.0
145.3 (**B_{3u}**,IR)	132.0 (**E″**,R)	135			132.0
142.3 (**A_g**,R)	129.2 (**A_1'**,R)		130 (R)		129.2
114.5 (**B_{2g}**, R)	128.9 (**A_2'**)				128.9
72.2 (**B_{2u}**,IR)	100.7 (**E′**,IR/R)				100.7
71.4 (**A_u**)	86.1 (**A_1''**)				86.1
50.4 (**B_{1u}**,IR)	75.2 (**A_2'**)				75.2
38.5 (**B_{2g}**,R)	64.6 (**E′**,IR/R)				64.6
	25.1 (**A_2''**,IR)				25.1
	18.7 (**E″**,R)				18.7

4.2. Thermodynamic properties of gaseous niobium fluoride species

The molecular parameters and the vibrational frequencies of the molecules calculated in this work were used as input for the determination of the thermodynamic properties of the gaseous species via statistical mechanical calculations. In order to extend the calculations to high temperature, additional information on the excited electronic levels of these molecules are required. In the present work, the calculations were performed over a temperature range from 298.15 K to 3000 K and the contribution of all the electronic terms below 30000 cm^{-1} was included. The effect of the ligand field was neglected in first approximation and the electronic energy levels of Nb^{+}, Nb^{2+}, Nb^{3+}, Nb^{4+} and Nb^{5+}, as given by Moore [45], were considered for the corresponding niobium fluorides.

The code calculates the temperature dependent thermodynamic functions, i.e. $S(T)$, $H(T)-H(298)$, $C_p(T)$ and $-(G-H(298))/T$, as well as the electronic, vibrational, rotational and translational contributions to the total value. A summary of the thermodynamic properties calculated in this work and used for the assessment is given in Table 7. The enthalpies of formation at 298.15 K of the lower niobium fluorides were calculated ab-initio while the values for the pentafluoride and its polymeric species were optimized during the assessment.

4.3. Thermodynamic assessment

The assessment of the binary Nb-F system has been performed in this work taking into consideration all the available experimental data on both the condensed and the gaseous phases, which are summarized in Table 8.

The enthalpy of formation of NbF_4(cr) and NbF_3(cr) were optimized to correctly reproduce the experimental observations on their thermal stability. NbF_4 was reported [10, 46] to be stable to approximately 523 - 623 K "under conditions which mantain NbF_5 pressure of few hundred microns" ($\simeq 6.6\cdot 10^{-4}$ bar). At higher temperatures, disproportionation takes place and proceed according to the reaction:

$$2NbF_4(cr) \longrightarrow NbF_3(cr) + NbF_5(g). \quad (6)$$

These observations are reasonably consistent with an atmospheric (1 bar total) disproportionation temperature of 790 K corresponding to the enthalpy of formation $\Delta_f H(NbF_4, cr, 298\ K)$=-1517.67 $kJ\cdot mol^{-1}$. Similarly, the enthalpy of formation of NbF_3 can be inferred from the observation of Ehrlich et al. [11]. The authors reported a sublimation temperature of 843 K in vacuum ($\simeq 1.3\cdot 10^{-6}$ bar), which is consistent with an atmospheric sublimation temperature of 1458 K and an enthalpy of formation of $\Delta_f H(NbF_3, cr, 298\ K)$=-1176.91 $kJ\cdot mol^{-1}$.

The second set of experimental data used for the optimization concerns the phase equilibrium in stoichiometric NbF_5. The total vapour pressure over pure NbF_5(cr, l) was measured both by Fairbrother and Frith [6] and by Junkins et al. [7] and their results agree very well, although no partial pressures of the monomer and

Table 7: The thermodynamic properties $\Delta_f H^0(298)$ (kJ·mol^{-1}), $S^0(298)$ (J·K^{-1}·mol^{-1}) and C_p(J·K^{-1}·mol^{-1}) of the gaseuous niobium fluorides in the temperature range 298.15–3000 K.

Compound	Δ_f**H**^{0}**(298)**	**S**^{0}**(298)**	**C**$_p$				
			a	b·T	c·T^{-2}	d·T^2	e·T^3
NbF(g)	235.76	239.86	37.846	$5.410\cdot10^{-3}$	$-1.375\cdot10^{5}$	$-1.845\cdot10^{-6}$	$3.045\cdot10^{-10}$
NbF_2(g)	-338.66	284.71	64.463	$-2.330\cdot10^{-3}$	$-9.302\cdot10^{5}$	$-3.321\cdot10^{-7}$	$1.732\cdot10^{-10}$
NbF_3(g)[a]	-804.41	300.25	124.879	$-2.440\cdot10^{-2}$	$1.931\cdot10^{6}$	$6.799\cdot10^{-6}$	$-6.737\cdot10^{-10}$
NbF_4(g)[b]	-1296.46	331.76	143.667	$-1.918\cdot10^{-2}$	$1.905\cdot10^{6}$	$4.495\cdot10^{-6}$	$-3.858\cdot10^{-10}$
NbF_5(g)	-1720.25	346.86	121.254	$1.596\cdot10^{-2}$	$-1.942\cdot10^{6}$	$-7.436\cdot10^{-6}$	$1.142\cdot10^{-9}$
Nb_2F_{10}(g)	-3531.16	534.92	261.303	$2.902\cdot10^{-2}$	$-4.027\cdot10^{6}$	$-1.352\cdot10^{-5}$	$2.078\cdot10^{-9}$
Nb_3F_{15}(g)	-5334.84	731.65	400.55	$4.275\cdot10^{-2}$	$-5.990\cdot10^{6}$	$-1.971\cdot10^{-5}$	$2.993\cdot10^{-9}$

[a] Additional C_p term: -21354.8 $\mathbf{T^{-1}}$
[b] Additional C_p term: -21676.7 $\mathbf{T^{-1}}$

Table 8: Available data for the phase diagram optimization.

Type of data	**Literature**	**Calculated**
NbF_3 sublimation (P$\simeq 1.3\cdot10^{-6}$ bar)	843 K [11]	843 K
NbF_4 disproportionation (P$\simeq$ 6.6$\cdot$ 10^{-4} bar)	523-623 K [10, 46]	573 K
NbF_5 boiling point	508 K [6], 506.5 K [7]	506.5 K
NbF_5 (cr,l) vapour composition	see Figure 3	
NbF_5 (cr,l) vapour pressure	see Figure 5	

the polymeric species could be determined. The composition in the gas phase and the relative amounts of monomeric and associated species were established by Boghosian et al. [21] based on the analysis of the Raman spectra at different temperatures. They observed a composition inversion, from polymers to monomers, at 573 K and calculated the stoichiometric coefficient for the association reaction $n\ NbF_5(g) \rightleftharpoons (NbF_5)_n(g)$ to be $n = 2$ in the complete temperature range 525–700 K.

Particular emphasis was placed in this work on the correct selection of the gaseous species present at equilibrium that need to be included in the database. This is especially important for a reliable determination of the thermodynamic properties of those species which are optimized during the assessment. In order to resolve the existent discrepancies of literature, three different thermodynamic models were tested in this work and were compared with the available literature data. The models differ in the degree of association of the pentafluoride in the vapour phase: NbF_5 and Nb_2F_{10} (Option I), NbF_5 and Nb_3F_{15} (Option II) and NbF_5, Nb_2F_{10} and Nb_3F_{15} (Option III), respectively. The first option, which follows the interpretation of Boghosian et al. [21], is in disagreement with the low temperature data ([19] at 333 K, [20] at 428 K) and the analysis of the IR spectra ([18] at 320 K) combined with our DFT calculations, that clearly shows trimeric association. On the other hand, option II does not correctly reproduce the data on vapour fractions and the stoichiometric coefficient measured by Boghosian et al. [21] at higher temperature. A slightly more complicated model is therefore proposed and considers all the three species NbF_5, Nb_2F_{10} and Nb_3F_{15} at equilibrium. The standard enthalpies of formation of the three species were optimized in this work to reproduce the best the experimental observations and the calculated fractions in vapour are shown in Figure 3. At low temperature (320–500 K) the trimer is the major species but, as the temperature increases, the predominant species shift from trimer to dimer at 519 K and from dimer to monomer at 552 K. The experimental data as measured by Boghosian et al. [21] are also reported in Figure 3 and compare very well with the calculated curves for the monomers and the polymers (dimers plus trimers). We note here that accordingly to the vapour pressure calculation method described in details in [47], these curves can be directly compared with the experimental data regardless of the association degree. While the partial pressure of the monomers is calculated directly from the intensity of the 727 cm^{-1} band, the partial pressure of the associate species is obtained as difference between the total system pressure and the monomer pressure.

It is also important to mention that according to our calculations all the pentafluoride species, and not only the monomer, have a Raman active mode around 727 cm^{-1}. A sum of several contributions to this intensity is therefore most likely, particularly in the low temperature range in which the concentration of dimeric and trimeric species is higher. This effect could lead to a deviant value for the stoichiometric coefficient of the associate reaction when this is calculated as the ratio of two Raman intensities at different temperatures. In the present case, the definition of a stoichiometric coefficient is not straightforward and a better indication of the degree of

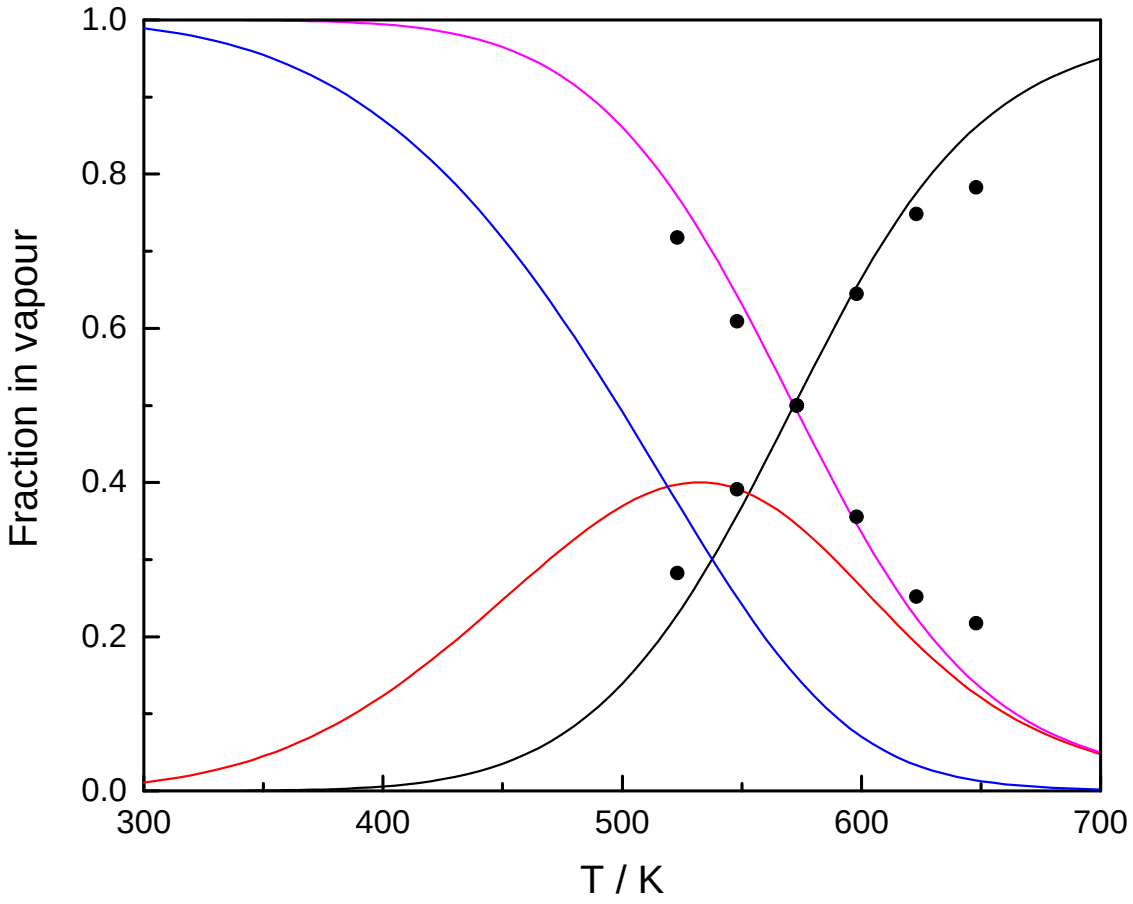

Figure 3: Relative amounts of the main gaseous species involved in the equilibrium above stoichiometric NbF_5. The solid lines correspond to the calculated fraction in vapour for the monomer (black), the dimer (red), the trimer (blue) and the polymers (pink) as obtained from the thermodynamic model developed. • Data by Boghosian et al. [21].

association of the pentafluoride as function of temperature is given by the apparent molecular weight of the gas phase. The calculated values, obtained combining the molar mass and the fraction of the species at equilibrium, are shown in Figure 4 and are compared with the experimental data by Alexander et al. [16]. Although the data were not directly used to optimise the thermodynamic model, they agree rather well with the predictions.

As shown above, the enthalpies of formation of the NbF_5, Nb_2F_{10} and Nb_3F_{15} gaseous species were optimized in this work to reproduce, as closely as possible, the vapor composition data and the NbF_5 boiling temperature. It was however not possible to reproduce the vapour pressure data [6, 7] without optimizing the NbF_5 enthalpy of fusion. Initially, the value measured by Brady et al. [12] was considered in the calculations but resulted in a significant divergence at low temperature (see dashed dotted line in Figure 5) close to the NbF_5 melting point. Although the vapour pressure is low in this region, direct measurements of the total pressure by static methods are usually quite accurate and the reproducibility of the data was confirmed in two independent studies. For this reasons, the enthalpy of fusion of NbF_5 was optimized in this work and a slightly higher value is proposed. The optimized enthalpy of fusion of 14.7 $kJ{\cdot}mol^{-1}$ provides a much better agreement with the experimental data (Figure 5) and could reasonably fit within the uncertainty of the measurements.

4.4. Phase diagram calculation

Based on the selected thermodynamic properties for the condensed and gaseous phases presented in this work, the phase diagram of the Nb-F system has been calculated and it is shown in Figure 6. The liquid phase (L) reported in the phase diagram is composed of nearly pure NbF_5(l), while the gas phase (G) is an ideal mixture containing many different species (NbF, NbF_2, NbF_3, NbF_4, NbF_5, Nb_2F_{10}, Nb_3F_{15}, F_2 and F). The relative concentrations strongly depends on temperature, as discussed throughout this paper, as well as fluorine content. As an example, we report in Figure 7 the calculated equilibrium composition of the vapour at the fixed temperature of 900 K. This is a key temperature value for the MSR design as it is considered as the reference operation temperature. Only the species with partial pressure above 10^{-12} Pa are indicated for clarity. As expected at high fluorine concentrations, only pure fluorine gases (F_2, F) and the pentafluorides species are important. However, at low fluorine concentrations, the lower niobium fluorides species start to play a role and substantially contribute to the equilibrium. An accurate description of these species, as provided in this work, is therefore required to correctly predict all the possible scenarios and to describe specific processes, such as the fluorination of niobium metal.

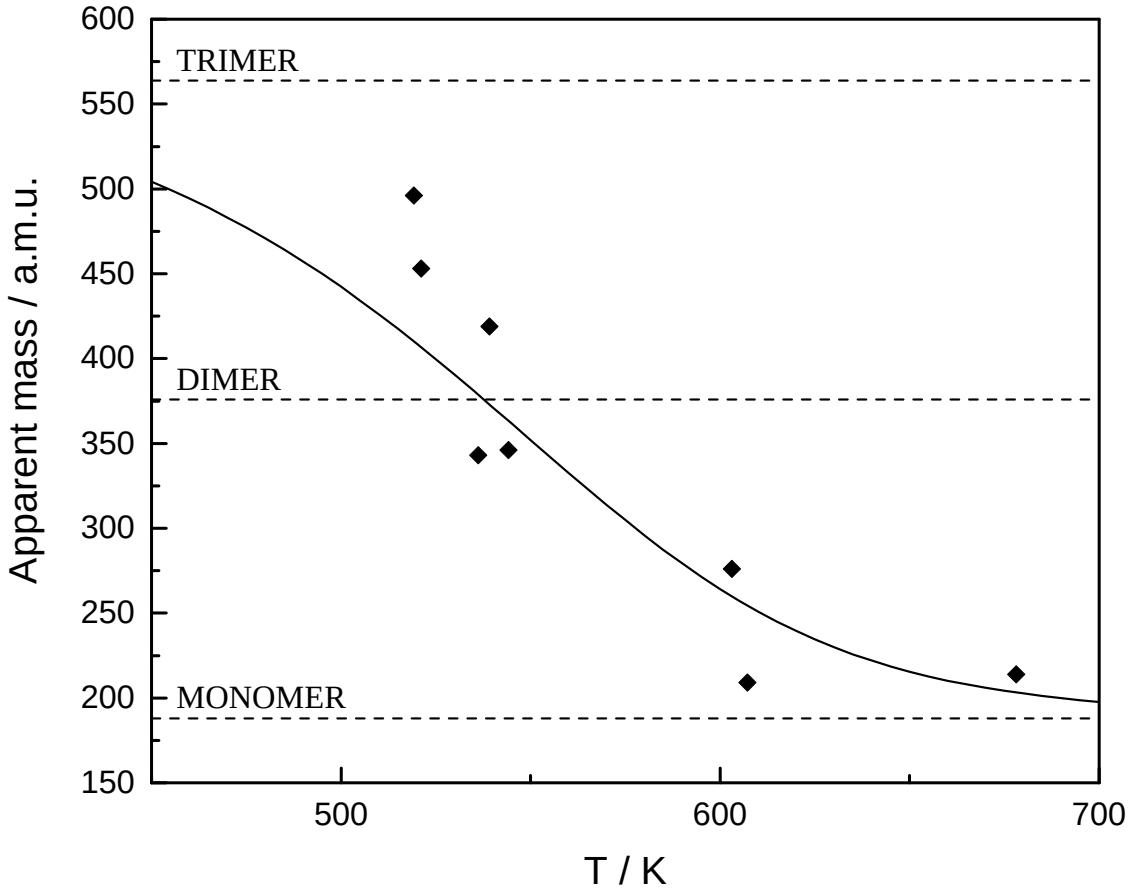

Figure 4: The calculated molecular weight of the gas-phase in stoichiometric NbF_5. ♦ Data from Alexander [16].

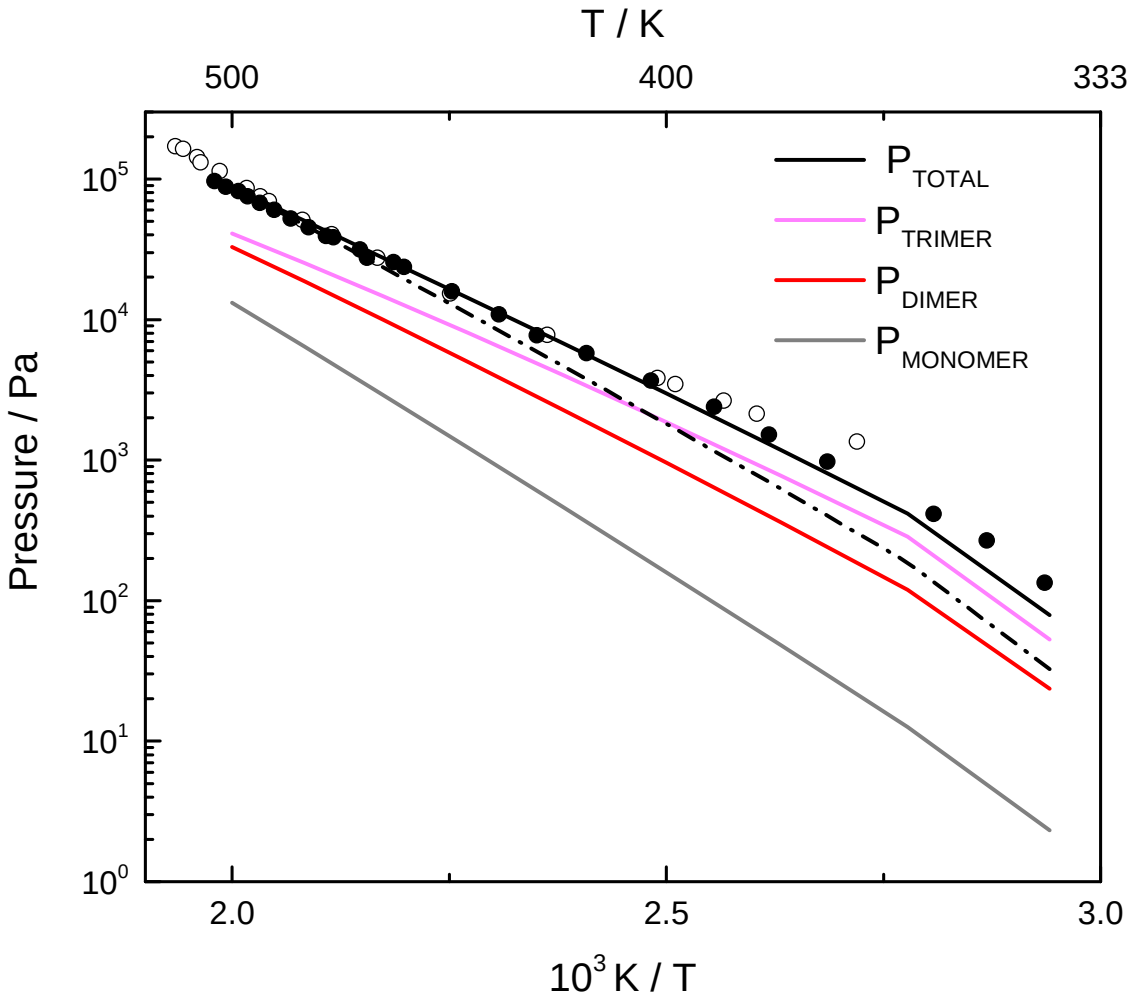

Figure 5: Vapour pressure of niobium pentafluoride NbF_5. The partial pressure of the monomer NbF_5 (grey line), the dimer Nb_2F_{10} (red line), the trimer Nb_3F_{15} (pink line) and the total pressure (solid black line) are calculated from the data selected in the proposed model. For comparison, the total pressure as calculated using the enthalpy of fusion as measured by Brady et al. [12] is also shown (dashed dotted line). ▲ Data from Junkins et al. [7]. ∘ Data from Fairbrother and Frith [6].

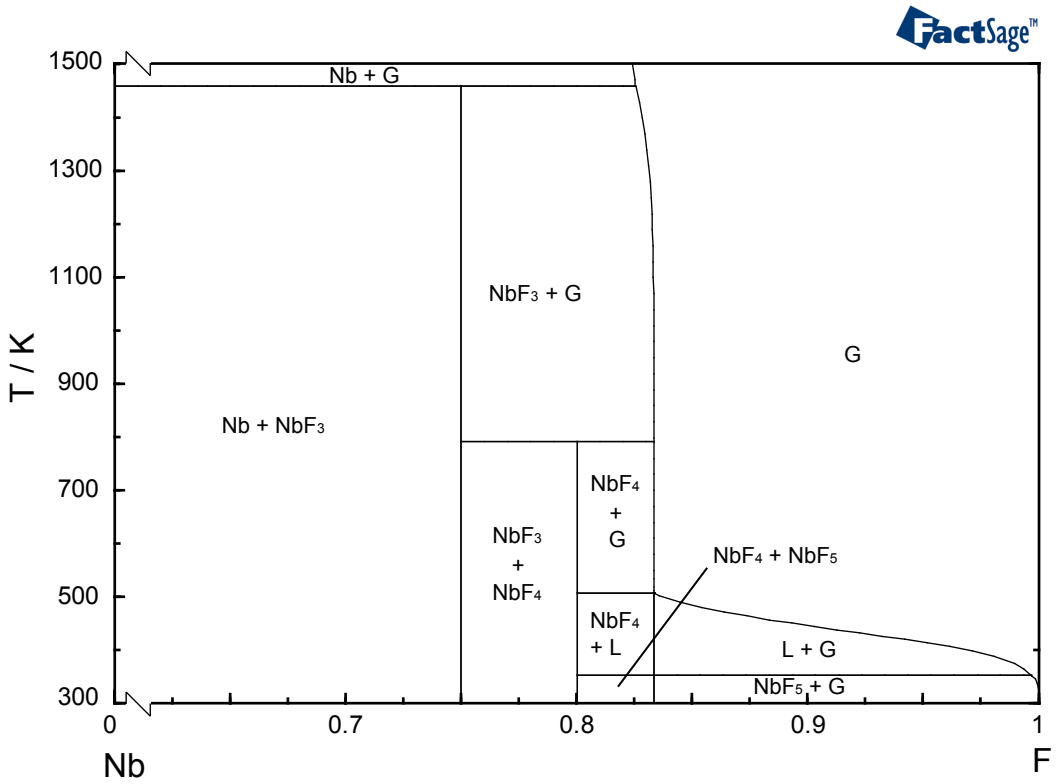

Figure 6: The phase diagram of the Nb-F system.

5. Conclusions

The available data on the thermodynamics of the niobium-fluorine system were firstly reviewed in this work. Although, three solid phases (NbF_3, NbF_4 and NbF_5) were found to be stable, only the pentafluoride was sufficiently studied. Similarly for the gaseous phase, a consistent and complete thermodynamic description of the different species was not available.

A combination of DFT and statistical mechanical calculations was applied in this work to provide novel thermodynamic data for the gaseous species. As first step, the molecular structure of all the niobium fluoride gas molecules and their harmonic vibrational modes were determined using DFT. The parameters were then used to estimate the standard entropy data and the temperature dependent heat capacity data presented in this paper.

The thermodynamic assessment of the niobium-fluorine system was performed according to the CALPHAD approach and taking into account the novel data. Different models were tested in this work to resolve the disagreement on the polymerization properties of niobium pentafluoride. It was concluded that all the associate species of the pentafluoride (i.e. monomer, dimer and trimer) are required to correctly describe the system and reproduce the available experimental data. Moreover, a new

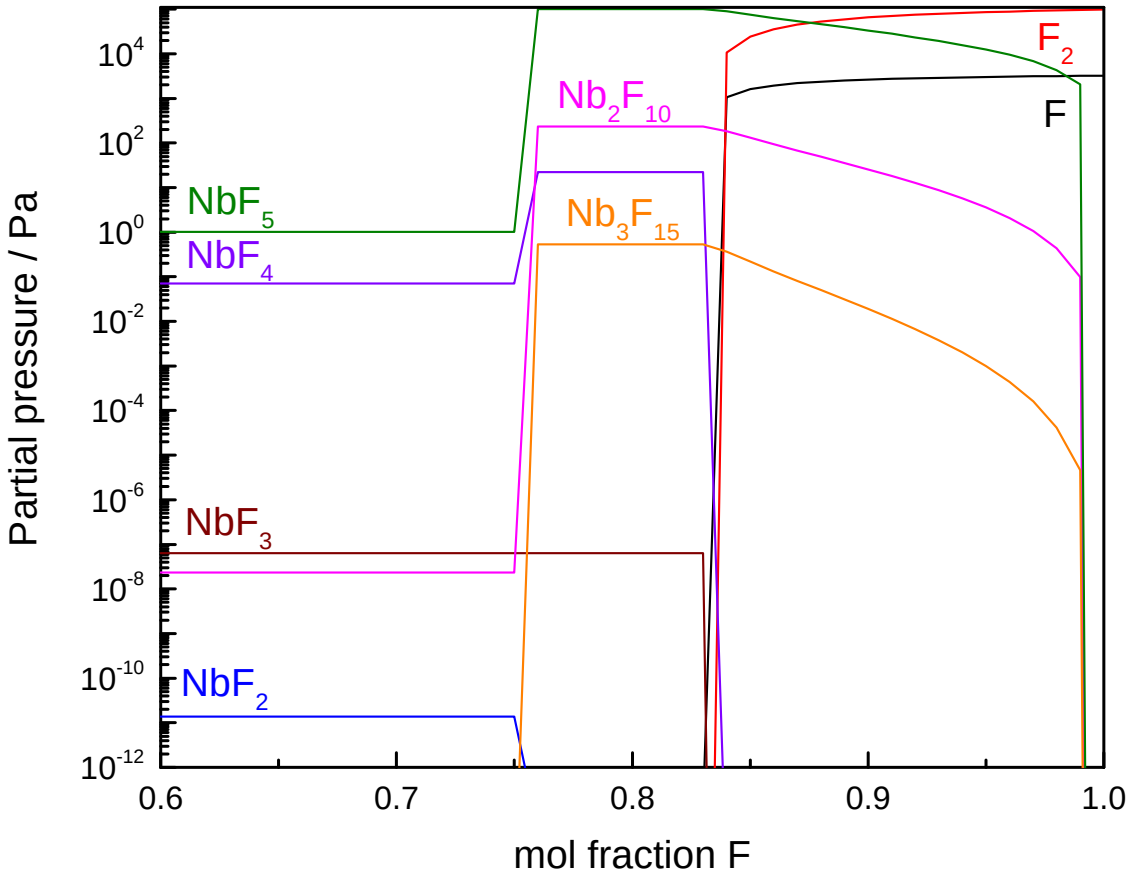

Figure 7: The calculated equilibrium composition of the gas phase as function of the fluorine concentration at 900 K.

value for the enthalpy of fusion of pure NbF_5 is proposed based on the thermodynamic model developed.

The thermodynamic assessment presented here reconciled all the literature data available on the Nb-F system and provide a consistent set of thermodynamic data. Nevertheless, further experiments are recommended to confirm the thermodynamic properties of the solid niobium fluoride compounds estimated in this work. Similarly, novel experimental data on the vapor species activities at low fluorine concentrations should be used to further validate the developed model. One of the most useful applications of the developed model is the calculation of the Nb-F phase diagram, which is presented in this work as well. It is a useful tool which permits the prediction of the most stable form of niobium in fluorine-containing environment as function of the temperature and the fluorine potential of the system.

Acknowledgments

The research forms part of the Dutch programme on Molten Salt Reactor Technology, funded by the Ministry of Economic Affairs. The authors would like to thank A. Kovács for the fruitful discussion on DFT calculations.

[1] A. Agulyansky, The chemistry of tantalum and niobium fluoride compounds, Elsevier, 2004.

[2] J. Serp, M. Allibert, O. Beneš, S. Delpech, O. Feynberg, V. Ghetta, D. Heuer, V. Ignatiev, J. L. Kloosterman, L. Luzzi, E. Merle-Lucotte, J. Uhliř, R. Yoshioka, D. Zhimin, Prog. Nucl. Energ. 77 (2014) 308–319.

[3] O. Beneš, R. J. M. Konings, Comprehensive Nuclear Materials, vol. 3, Elsevier Inc., 359–389, 2012.

[4] R. G. J. Ball, B. R. Bowsher, E. H. P. Cordfunke, S. Dickinson, R. J. M. Konings, J. Nucl. Mat. 201 (1993) 81–91.

[5] E. H. P. Cordfunke, R. J. M. Konings, J. Nucl. Mat. 201 (1993) 57–69.

[6] F. Fairbrother, W. C. Frith, J. Chem. Soc. (1951) 3051–3056.

[7] J. H. Junkins, R. L. Farrar, E. J. Barber, H. A. Bernhardt, J. Am. Chem Soc. 74 (1952) 3464–3466.

[8] A. Edwards, J. Chem. Soc. (1964) 3714–3716.

[9] L. M. Toth, G. P. Smith, Tech. Rep. ORNL-4229, 1967.

[10] F. P. Gortsema, R. Didchenko, Inorg. Chem. 4 (1965) 182–186.

[11] P. Ehrlich, F. Ploger, G. Pietza, Z. Anorg. Allg. Chem. 282 (1955) 19–23.

[12] A. P. Brady, O. E. Myers, J. K. Clauss, J. Phys. Chem. 64 (1960) 588–591.

[13] E. Greenberg, C. A. Natke, W. Hubbard, J. Phys. Chem. 69 (1965) 2089–2093.

[14] O. E. Myers, A. Brady, J. Phys. Chem. 64 (1960) 591–594.

[15] C. F. Weaver, J. W. Gooch, H. A. Friedman, J. D. Redman, Tech. Rep. ORNL-4396, 1969.

[16] L. E. Alexander, I. R. Beattie, P. J. Jones, J. Chem. Soc. Dalton Trans (1971) 210–212.

[17] H. Preiss, Z. Anorg. Allg. Chem. 389 (1972) 280–292.

[18] R. J. M. Konings, Struct. Chem. 5 (1994) 9–13.

[19] J. Brunvoll, A. A. Ischenko, I. N. Miakshin, G. V. Romanov, V. P. Spiridonov, T. G. Strand, V. F. Sukhoverkhov, Acta Chem. Scand. A34 (1980) 733–737.

[20] I. S. Gotkis, A. V. Gusarov, L. N. Gorokhov, Russ. J. Inorg. Chem. 20 (1975) 702–705.

[21] S. Boghosian, E. A. Pavlatou, G. N. Papatheodorou, Vib. Spectrosc. 37 (2005) 133–139.

[22] E. L. Voit, A. V. Voit, V. K. Goncharuk, V. I. Sergienko, J. Struct. Chem. 40 (1999) 509–514.

[23] D. D. Wagman, W. H. Evans, V. B. Parker, R. H. Schumm, I. Halow, S. M. Bailey, K. L. Churney, R. L. Nuttall, J. Phys. Chem. Ref. Data 11.

[24] I. Barin, O. Knacke, O. Kubaschewski, Thermochemical Properties of Inorganic Substances, Springer-Verlag, Berlin, 1977.

[25] N. P. Galkin, Main properties of inorganic fluorides. Handbook (in Russian), Atomisdat, Moscow, 1976.

[26] A. Glassner, Tech. Rep. ANL-5750, 1957.

[27] R. C. Feber, Tech. Rep. LA-3164, 1965.

[28] N. P. Galkin, V. N. Tumanov, V. P. Korobstev, G. A. Batarev, V. A. Pavlov, Russ. J. Phys. Chem. 45 (1971) 1532.

[29] C. W. Bale, E. Bélisle, P. Chartrand, S. A. Decterov, G. Eriksson, K. Hack, I. H. Jung, Y. B. Kang, J. Melançon, A. D. Pelton, C. Robelin, S. Petersen, CALPHAD 33 (2009) 295–311.

[30] M. W. Chase Jr.(ed.), NIST-JANAF Thermochemical Tables Fourth Edition, J. Phys. Chem. Ref. Data, Monograph 9.

[31] R. Guillaumont, T. Fanghänel, V. Neck, J. Fuger, D. A. Palmer, I. Grenthe, M. H. Rand, Update on the Chemical Thermodynamics of Uranium, Neptunium, Plutonium, Americium and Technetium, vol. 5, Chemical Thermodynamics, OECD Nuclear Energy Agency, 2003.

[32] O. Beneš, J. C. Griveau, E. Colineau, D. Sedmidubsky, R. J. M. Konings, Inorg. Chem. 50 (2011) 10102–10106.

[33] E. H. P. Cordfunke, R. J. M. Konings, J. Phase Equilib. (1993) 457–464.

[34] M. J. Frisch, G. W. Trucks, H. B. Schlegel, G. E. Scuseria, M. A. Robb, J. R. Cheeseman, G. Scalmani, V. Barone, B. Mennucci, G. A. Petersson, H. Nakatsuji, M. Caricato, X. Li, H. P. Hratchian, A. F. Izmaylov, J. Bloino, G. Zheng, J. L. Sonnenberg, M. Hada, M. Ehara, K. Toyota, R. Fukuda, J. Hasegawa, M. Ishida, T. Nakajima, Y. Honda, O. Kitao, H. Nakai, T. Vreven, J. A. M. Jr., J. Peralta, F. Ogliaro, M. Bearpark, J. Heyd, E. Brothers, K. Kudin, V. N. Staroverov, T. Keith, R. Kobayashi, J. Normand, K. Raghavachari, A. Rendell, J. Burant, S. Iyengar, J. Tomasi, M. Cossi, N. Rega, J. M. Millam, M. Klene, J. E. Knox, J. Cross, V. Bakken, C. Adamo, J. Jaramillo, R. Gomperts, R. Stratmann, O. Yazyev, A. J. Austin, R. Cammi, C. Pomelli, J. Ochterski, R. L. Martin, K. Morokuma, V. G. Zakrzewski, G. A. Voth, P. Salvador, J. J. Dannenberg, S. Dapprich, A. D. Daniels, O. Farkas, J. B. Foresman, J. V. Ortiz, J. Cioslowski, D. J. Fox, Gaussian 09, Revision B.01, Gaussian, Inc., Wallingford CT, 2010.

[35] A. D. Becke, Phys. Rev. A: At., Mol., Opt. Phys 38 (1988) 3098–3100.

[36] C. Lee, W. Yang, R. G. Parr, Phys. Rev. B: Condens. Matter Mater. Phys. 37 (1988) 785–789.

[37] S. Riedel, M. Kaupp, Coord. Chem. Rev. 253 (2009) 606–624.

[38] D. Andrae, U. Haeussermann, M. Dolg, H. Stoll, H. Preuss, Theor. Chim. Acta 77 (1990) 123–141.

[39] J. M. L. Martin, A. Sundermann, J. Chem. Phys. 114 (2001) 3408–3420.

[40] T. H. Dunning, J. Chem. Phys. 90 (1989) 1007–1023.

[41] J. W. Ochterski, Gaussian white paper "Thermochemistry in Gaussian", 2000.

[42] A. R. Allouche, J. Comp. Chem. 32 (2011) 174–182.

[43] S. Blanchard, J. Chim. Phys. (1965) 919–920.

[44] N. Acquista, S. Abramowitz, J. Chem. Phys. 56 (1972) 5221–5224.

[45] C. E. Moore, Atomic Energy Levels, Tech. Rep. NSRDS-NBS 35, 1971.

[46] C. F. Weaver, J. S. Gill, J. D. Redman, Tech. Rep. ORNL-4782, 1972.

[47] S. Boghosian, G. N. Papatheodorou, J. Phys. Chem. 93 (1989) 415–421.